IIBCC 2010
International Inorganic-Bonded Fiber Composites Conference

APPLICATION OF DFRCC THIN BOARD TO PASSIVE-VIBRATION-CONTROL PANEL FOR WOODEN FRAMES

KANJI YAMADA, AYUMI SATOH and SATORU ISHIYAMA

Akita Prefectural University: Tsuchiya, Yurihonjo, Akita, 015-0055, JAPAN

ABSTRACT

The authors investigate the application of highly ductile fibre reinforced cement composites (DFRCC) as a passive-vibration-controlled aseismatic device for wooden frames.

In this study, experiments were conducted with various types of wooden frames filled with DFRCC panels. They include 7 frames filled with commercial DFRCC boards having various types of incisions to induce multiple cracks to dissipate seismic vibration energy.

The structural behaviours of the frames were observed while repeatedly applying gradually increasing drift angle from 1/480 radian finally up to 1/30 radian.

The experimental results showed that the damping factor of a frame made of DFRCC panel with incisions was 34% due to induced cracks in it, whereas those of the reference panels were about 11% at the highest. From these values, the expected response load for this type of DFRCC panels would be substantially reduced.

KEYWORDS:

Ductile Fibre Reinforced Cement Composites; Passive-Vibration-Control; PVA fibre.

INTRODUCTION

There are many techniques and principles for designing wooden structures to be earthquake-resistant. One of the newest ideas for such issues is passive control of the earthquake vibrations by applying energy dissipation devices (JSSI, 2003). These mitigate seismic load by increasing the natural period of the structure and by making the response acceleration smaller due to their high damping factor (h_{eq}).

There are some experimental studies in which velocity dependent dampers or displacement dependent dampers were evaluated for wooden frames. Kasai (Kasai, 2004) evaluated 6 dampers in wooden frames (width 0.9m) where cyclic loading was applied. Sakata (Sakata, 2004) evaluated 5 dampers in wooden frames (width 2.73m) where the same acceleration as measured in a real earthquake was applied through an acceleration platform. Ooki (Ooki, 2004) also evaluated 2 dampers in steel frames. The performance of these dampers is 260 – 360 kN-mm (Kasai, 2004) in dissipated energy in a cycle at 1/120 rad, or 27 – 30 tf-s/cm (Sakata, 2004) in C_{eq} (damping coefficient). If such dampers are evaluated in a frame, the damping factor h_{eq} is as high as 12% (Ooki, 2004).

The authors have been studying a special type of DFRCC (ductile fibre reinforced cement composites) that has a great capacity of fracture energy dissipation due to multiple cracking in the material (Yamada, 2005 2006). If the material is used for this new type of panels, it can be a substitutable element for mitigating seismic damage, establishing a new application for DFRCC. In this paper, we describe some experimental findings from the study of the vibration energy dissipation panel but we exclude the theoretical part of the study which is shown in the reference (Yamada, 2008).

EXPERIMENTS

Properties of DFRCC board

The DFRCC board used for our experiments is commercial DFRCC board (Ogawa, 2005) which is a thin cementitious composites manufactured on the Hatcheck Process Machine, containing 3% of PVA (polyvinyl alcohol) fibre. We obtained the tensile strength and fracture energy from an inverse analysis using the results of the fracture toughness test. The mechanical properties of the dried DFRCC board so obtained are 17.78 MPa for tensile strength and 6.08 N/mm for fracture energy, but when wet, the values are 8.9 MPa and 7.77 N/mm respectively, demonstrating that the fracture energy is the greatest when the board is wet and the least when dried. The room dried board has intermediate values for both strength and energy, which one can see in Fig.1. The dependency of the mechanical properties to the water content is usual for fibre reinforced cementitious thin board.

Fracture modes

Modelling of the wooden frame with DFRCC for FEM analysis must include three material factors; viz. type of wood, FRC board and the fasteners. The fasteners tend to laterally sink into FRC board and into wood as well, which makes the analysis of the total rigidity of the wall difficult. The analysis of the cracks around incisions in the board was successful and Fig. 2 represents a part of the crack pattern analysed with FEM analysis superimposed on the experimental FRC board after the fracture test of structure HS.

The authors established the following equations for estimating the fracture load of the structure according to the three fracture modes; tensile fracture of the board, buckling fracture of the board due to the compression by shear force and the fracture around the board fasteners. They include empirical factors determined from experiments with the elements and FEM analyses. Equations (1) to (3) are based on those used for the design of steel girders under heavy shear load.

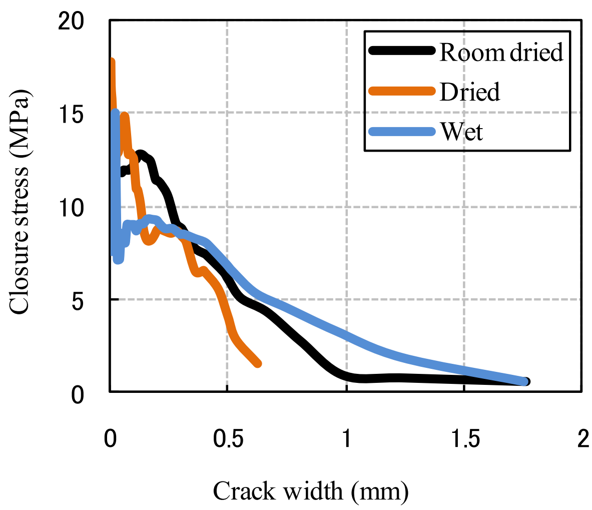

Figure 1– Tension softening diagram of DFRCC.

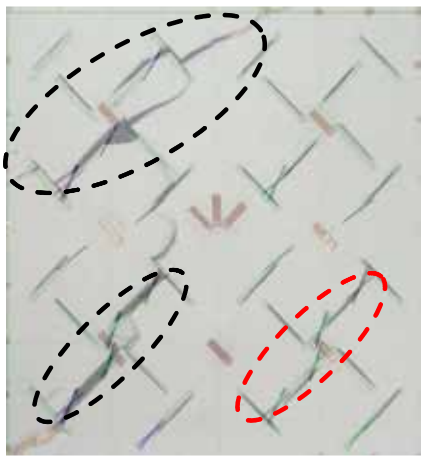

Figure 2– A part of crack pattern after fracture.

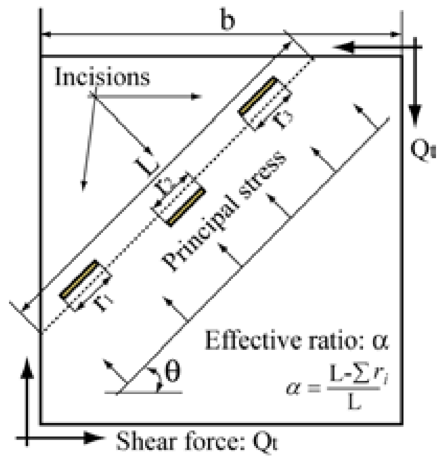

Figure 3 – How to calculate α.

Fracture load of the wall

(1) Tensile fracture of the board

$$Q_t = \sigma_t \cdot b \cdot \alpha \cdot t \cdot \sin\theta \cos\theta \quad (1)$$

Where, Q_t is tensile fracture load of the board, σ_t is the strength of the FRC board, b is the length of the board, α is the effective ratio of the board which varies with the ratio of the incisions in the board, t is the thickness of the board and θ is 45°. The ratio α is calculated as shown in Fig.3.

(2) Buckling fracture of the board

$$Q_{cr} = \tau_{cr} \cdot b \cdot \beta \cdot t \tag{2}$$

$$\tau_{cr} = \left(5.34 + \frac{4.00}{\left(a/b\right)^2} \right) \cdot \frac{\pi^2 E}{12(1-\nu^2)} \cdot \frac{1}{(b/t)^2} \tag{3}$$

Where, Q_{cr} is buckling fracture load of the board, τ_{cr} is buckling stress of the board, β is the factor of the reduction by the incisions, E is Young's modulus of the board, ν is Poisson's ratio, a is the width of the board, and t and b are the same as the equation (1).

(3) Fracture around the fastener

$$Q_s = nQ_{s1} / \gamma \tag{4}$$

Where, Q_s is the total bearing load against lateral deformation and splitting of the board around the fastener, n is the number of the fasteners, Q_{s1} is the bearing load per a fastener determined by experiment and γ is an empirically determined factor from the experimentation.

Tested wall structures

The authors conducted experiments in which nine types of real-dimensioned wall frames were tested. The outline of test setup is represented in Fig. 4. The frame was laid down and load was applied laterally. Load and displacement at 8 major joints were recorded repeatedly along with the loading cycles. Also the strain at major points in frames and board was measured. The drift angle for the cyclic loading starts with 1/480 rad and it was gradually increased until reaching a value of 1/30 rad of drift angle.

The features of test frames are shown in Table 1. F2 and F3 type structures are basic frames consisting only of wooden beams and columns that are made of cedar without a cladding inside the frame. These were bare frames for the reference. All other frames were filled with various claddings of DFRCC board, in which there were many distributed incisions for inducing cracks that would absorb applied vibration energy. (See Fig. 5.)

HS and HA type structures have uniformly distributed incisions by which concentrated tensile stress around the incisions due to shear force is expected to be almost the same. HT type structures have smaller incisions at the bottom of the wall for inducing sequential cracks from the top to the bottom of the wall. HO and HW structures have the same incisions constituting a 'truss mechanism' at the beginning before transforming to a 'rigid frame mechanism'. It means the 'truss mechanism' begins to break by the cracks of the cladding, but there were no cracks on the corner of it even when reaching a high value of drift angle. The corner of the wall rigidly connects the wooden columns and the beams eventually constituting the 'rigid frame mechanism'. HO differs from HW in water content of the DFRCC cladding; HO has room-dried board whereas HW is wet, i.e., the fracture energy of the board is different as described in the next section.

Table 1 – Outlined features of tested wall structures.

Type	Frame	Features
F2 and F3	-	Wooden frames without wall board (without stud (F2) or with studs (F3))
HS and HA	F2	Uniformly distributed incisions for widespread cracks
HT	F3	Uneven incisions for sequential crack development
HO	F3	Incisions arranged for constituting both truss and rigid frame mechanisms in dry board (HO) or in wet board (HW)
HW	F3	
M3VF	F3	Developed version of incisions from HO to have distributed cracks, and a better energy dissipation due to added FRP
M3.1VF	F3	

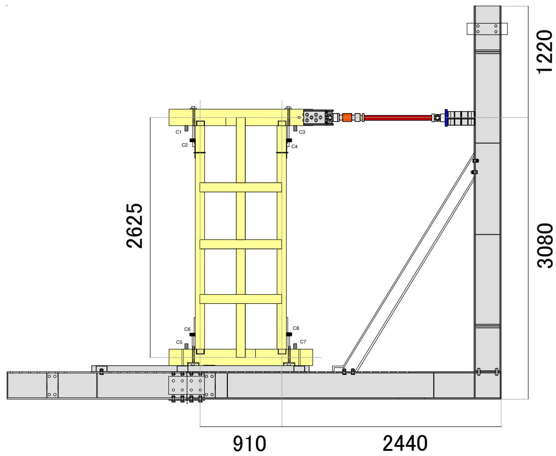

Figure 4 – Test setup for cyclic loading of wall.

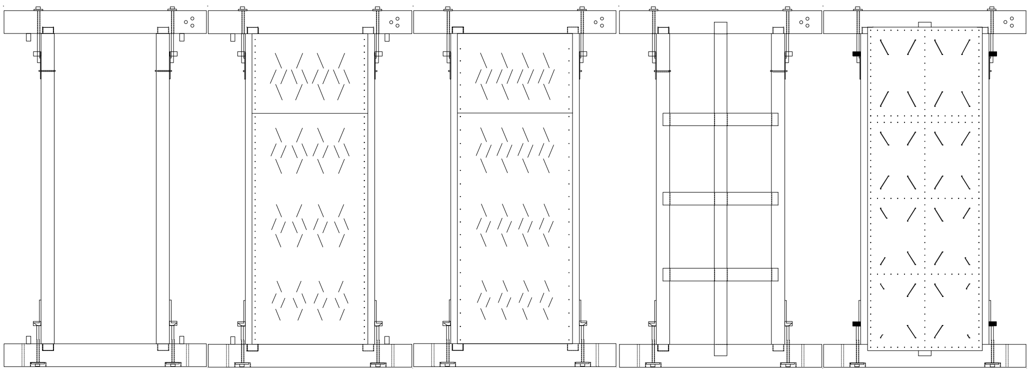

(A) F2 (B) HS (C) HA (D) F3 (E) HT

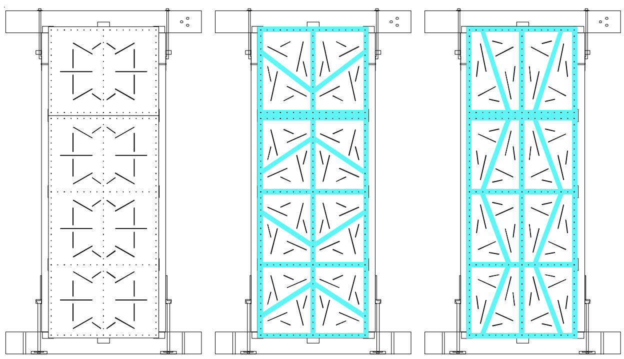

(F) HO and HW (G) M3VF (H) M3.1VF

Figure 5 – Tested wall structures with different incisions in the board.

RESULTS

Mode of fracture

The fracture of HA and HS occurred at the fasteners when the board buckled due to shear-force-induced compressive stress at about 10 kN (1/90 rad). This low buckling strength results from the large width-to-thickness ratio of the board, because the wooden frame F2 had no internal reinforcing studs within the frame. It is clear that to obtain high buckling load, the panel should be divided into small segments with studs, which one can see from equation (2).

The board in HT was strong enough to induce cracks in the bottom wooden beam and also a large subsidence around the hold-down fixture, which caused a large deformation. The reason that caused no cracks formed in the board is that slip around the fasteners restricted the shear force to be transferred to the board. This may be the case for ordinary wall filled with plywood or cement board that has no incisions in it.

As expected, HO had many cracks in the board which gradually decreased the rigidity of the frame. HW displayed no visible cracks in the cladding, but a decreased rigidity of the structure and a large strain exceeding the crack strain indicated the existence of invisible cracks, as demonstrated by the measurement of strain gauges attached to the board.

M3VF and M3.1VF had a good ductility maintaining load carrying capacity until large deformation resulted in the development of many cracks in the board. Added FRP (fibre reinforced plastics) strips worked as added columns and beams in the board. The fibre used in FRP was PVA fibre which broke when cracks propagated into the FRP. It may be more useful if the fibre were steel fibre for enhancing the ductility.

Restoring force characteristics and derivatives

Fig. 6 shows the resulted restoring force characteristics, and Table 2 the summary of the results. In Table 2, h_{eq} is a damping coefficient proportional to the absorbed energy within a load cycle which is associated with the advantage of absorbing vibration energy. The ductility factor (μ) in Table 2 was calculated from the envelope curve in Fig. 6, assuming the response behaviour is completely elastic-plastic. The wall multiplication factor (Wm) is a calculated factor based on the standard (AIJ, 2002) which shows the capability ratio of resisting shear force. Wm is 1.0 when shear force capacity is 1,960N per the projected lateral length of wall.

DISCUSSION

The performance of wall structures

The ordinary wall filled with plywood or cement board is known to have a value of 2.5 for the wall multiplication factor (Wm) stipulated in building standard law of Japan. But the Wm values for HO and HW that have incisions in the board have values above 19% (HO) or 34% (HW) greater than that of ordinary board with no incisions. This derives from their large ductility factors which come from the gradual fracture of the board.

The important point for HO and HW is that the incisions did not decrease initial rigidity due to the 'truss mechanism' finally allowing a large deformation after cracks occurred, which contributed to large μ . The mechanism of large deformation is due to the rigid frame mechanism consisting of wooden beams and columns connected with DFRCC board at the nodes. Though the inner board has many cracks and incisions, the nodes are free of cracks and incisions. So it can be said that HO and HW exhibited both mechanisms of truss and rigid frame. The detailed process of fracture is depicted in Fig. 7.

Table 2 shows that h_{eq} of HW is a value of 39% at 1/30 rad. It means that the response of shear force would be decreased to 30% of the input shear force based on the damping effectiveness coefficient (D_h) calculated with Equation (5). This would contribute to the safety of wooden frame which suffers a quite large earthquake. The same advantage is recognized at 1/120 rad telling that the response would be reduced to 45% of the input even at such a small drift angle due to large h_{eq} (23.2%).

$$D_h = 1.5 / (1 + 10 h_{eq}) \tag{5}$$

Where, D_h is damping effectiveness coefficient and h_{eq} is damping factor.

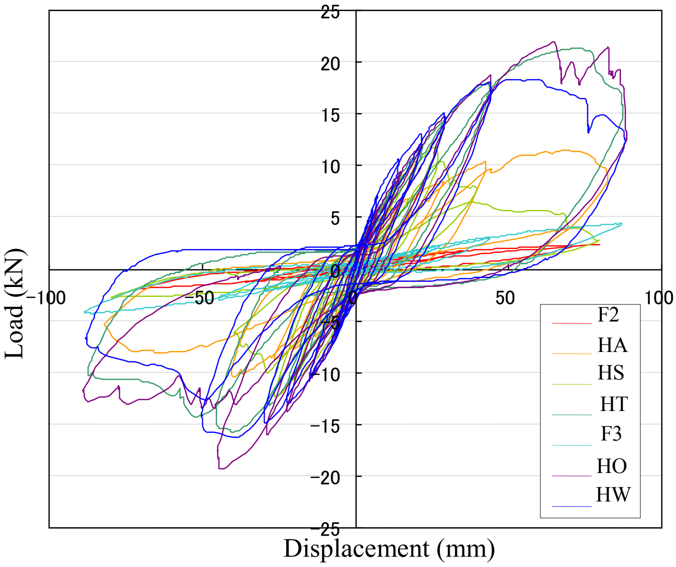

(A) Wall structures without added FRP strip.

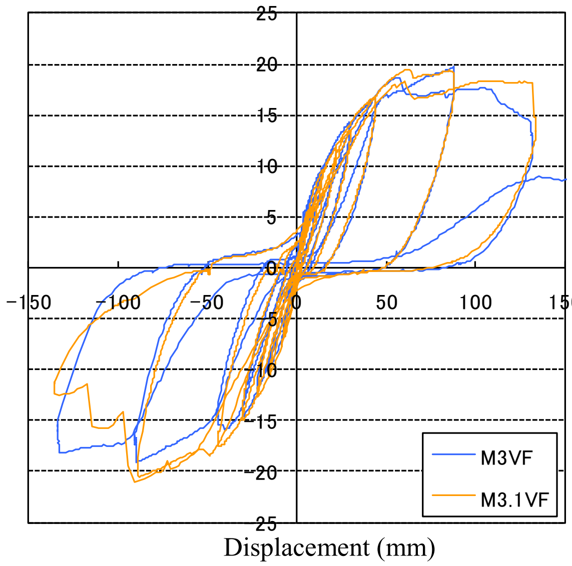

(B) Wall structures with added FRP strip.

Figure 6– Resulted restoring force characteristics.

Table 2– Summary of test results.

Type	Max. load (kN)	h_{eq} (%) 1/120 rad	h_{eq} (%) 1/30 rad	μ (-)	Wm (-)
HA	11.6	13.6	21.7	4.2	1.36
HS	11.8	10.0	31.3	2.0	2.04
HT	21.3	7.6	23.1	2.5	2.88
HO	21.9	7.7	23.9	2.6	2.99
HW	18.4	23.2	39.0	4.2	3.35
M3VF	19.7	9.1	19.7	3.85	3.64
M3.1VF	19.45	11.7	17.8	4.61	3.41

μ : Ductility factor, Wm: Wall multiplication factor.

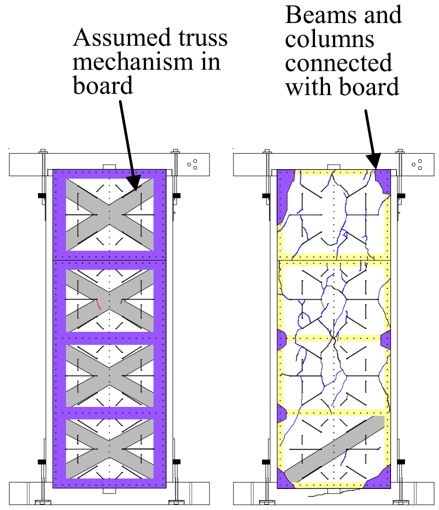

(A)Below 1/60 rad. (B) At 1/30 rad.

Figure 7– Fracture mechanisms.

Bi-linear models

Fig. 8 represents bi-linear models of all tested wall structures. It is obvious that M3VF and M3.1VF have a large zone of load carrying capacity, which develops a large ductility factor and consequently yields high Wm. This type of wall structure is useful for the aseismatic design of structure based on the structural design by strength criteria using Wm.

On the other hand, HO and HW have large h_{eq}, which means large absorption of seismic vibration energy. This type of wall structure is useful for the aseismatic design of structure using the passive-vibration-control mechanism, especially against huge earthquakes based on the limit state-design.

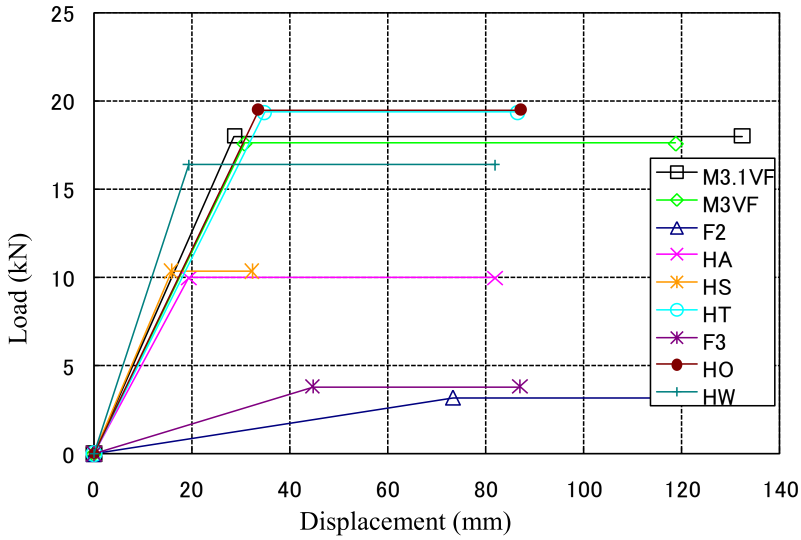

Figure 8– Bi-linear models of wall structures.

CONCLUSIONS

It is possible to make wooden frames earthquake resistant by using the HO or HW type of vibration energy dissipation panel proposed in this study. The values of wall multiplication factor are above 20% greater than that of the ordinary type wall conventionally used for wooden houses.

HO type panel has both truss and rigid frame mechanisms of resisting shear force, which leads to a large ductility factor and a high strength as well.

HW type panel absorbs large amounts of fracture energy, which leads to a large damping coefficient of about 39%. This value means that the respondent shear force would be reduced to 30% of the input.

M3VF and M3.1VF types have large ductility factors and Wm's, which derives from the added FRP strip and improved incisions. They are effective for the aseismatic structural design by strength criteria using Wm.

ACKNOWLEDGEMENTS

This study was financially supported by JSPS's Grant-in-aid for scientific research (C-18560555, 2006) and by JICE's Grant-in-aid (08001, 2008), which the authors express gratitude.

REFERENCES

AIJ, Standard for structural design of timber structures, AIJ, Tokyo, Japan, (2002), 352 pp.

JSSI (Japan Society of Seismic Isolation), 'Manual for Design and Construction of Passive Control Structure', Japan Society of Seismic Isolation, Tokyo, Japan, (2003), 405 pp.

Kasai, K., Wada, A., Sakata, H., Ooki, Y. and Miyashita, T., 'Passive Control for Mitigating Seismic Damage to Wood Houses: Part 1 Behavior and Design of Joints, Dampers and System', Proceedings of Passive Control Symposium 2004, Tokyo, Japan, Nov. 15-16 (2004), 169-184.

Ogawa, A., Hitomi, Y. and Hoshino, H., 'PVA-fibre reinforced high performance cement', Proceedings of the Intl. RILEM Workshop on HPFRCC in Structural Applications, (2005), (C-1-3),1-8.

Ooki, Y. Kasai, K., Wada, A., Midorikawa, M., Yokoyama, S. and Iwasaki, K., 'Passive Control of Light-Gage Steel Houses: Dynamic Loading Test, Shaking Table Test and Analysis', Proceedings of Passive Control Symposium 2004, Tokyo, Japan, November 15-16 (2004), 203-218.

Sakata, H., Kasai, K., Wada, A., Midorikawa, M., Ooki, Y. and Nakagawa, T., 'Passive Control for Mitigating Seismic Damage to Wood Houses: Part 2 Performance Validation and Comparison by Shaking Table Test', Proceedings of Passive Control Symposium 2004, Tokyo, Japan, Nov. 15-16 (2004), 185-201.

Yamada, K., Saijo, R., Furumura T. and Tanaka, S., 'Application of Extrusion Molded DFRCC to Permanent Form', Proceedings of the Intl. RILEM Workshop on HPFRCC in Structural Applications, (2005), 253-260.

Yamada, K., Sasaki, I. and Ishiyama, S., 'Performance of vibration energy dissipation panel made of highly ductile FRCC', Proceedings of 2nd Asian concrete federation conference, (2006), 226-236.

Yamada, K., Sasaki, I. and Ishiyama, S., 'A Discussion on Development of Seismic Energy Dissipation Wall for Wooden Frame Employing FRCC board', Proceedings of AIJ Tohoku Chapter Architectural Research Meeting, (2008), 71, 85-88.